

DENOISING OF MRI USING MODIFIED NON LOCAL MEAN FILTER

VANDANA V. HANCHATE^{1,*}, KALYANI R. JOSHI²

Progressive Education Society's, Modern College of Engineering, Pune, Maharashtra, India
*Corresponding Author: vnjpune@gmail.com

Abstract

This paper proposes a modified non local mean algorithm (MNLN) for removal of noise from MRI images and an implementation using the hardware platform Spartan 6 FPGA. The algorithm removes noise and as well preserves image details. The subjective and objective measures are calculated and analysed, which shows clearly the improvement of MNLN algorithm over conventional Non Local Mean (NLM) algorithm. Different quantitative measures related to structure and edge profile such as MSE, PSNR, SSIM and PFOM are proof for the maximum matching between original and denoised image. Algorithm is implemented on a Field Programming Gate Array (FPGA) platform. This implementation is time saving compared with conventional Matlab implementation and parallel processor implementation. Algorithm is also compared with bilateral filter which shows the advantages of proposed algorithm over all conventional algorithms.

Keywords: Bilateral filter, Field programming gate array, Image filtering, Non local mean filter, Pratt figure of merit, Structural similarity index.

1. Introduction

Magnetic Resonance Imaging (MRI) is helpful to doctors for diagnosing a disease and also it can be used to find out response given by the patient to current treatment. MRI can be done on different parts of the body such as brain, spinal cord, heart etc. It is helpful in diagnosis of cancer, brain injury, heart disease, multiple sclerosis etc. For diagnosis purpose, the object of interest for the doctor will be a tumour or a damaged tissue captured in MRI scan. But often MRI is contaminated with a noise called Rician noise. It is noise which is dependent on signal. It is a type of artefact which is introduced at the time of acquisition process of the MR images, making accurate imaging difficult. It produces random changes that cause additional bias to the MR images because of which image contrast decreases. It gives Rayleigh distribution in low intensity region whereas, changes to Gaussian distribution in high intensity region [1]. Removing Rician noise from the image without disturbing a structure is always a challenging task for the researchers. Different algorithms are proposed by different researchers. Comparison of different filters are presented in the survey paper [2] with its advantages and disadvantages.

Bilateral filtering [3] preserves image's edges by nonlinear combination of neighbouring pixel values. The main advantage of this method is that it is simple and non iterative. Geometric closeness and their photometric similarity are considered for combination of gray levels.

Unlike the local mean filter which takes the mean value of the local area surrounding the target pixel, non local means (NLM) [4] filtering take a weighted averaging of all the surrounding pixels in the image around the target pixel. The weight is decided by how similar this pixel is along with its neighbourhood with target pixel and its neighbourhood.

Block matching techniques with noise invalidation and variance stabilization techniques [5] shows denoising of MRI in wavelet domain. It is a combination of non local approach, 3D wavelet shrinkage and 3D Wiener filtering. Initially Rician noise is converted into Gaussian with the help of noise invalidation technique. Also, instead of hard thresholding, a soft thresholding technique is used using variance stabilization technique. Algorithm is tested using peak signal to noise ratio (PSNR) and structural similarity index measure (SSIM) quality metrics.

Akar [6] had introduced modified bilateral filter which is based on genetic algorithm (GA) for optimal parameter calculation. To find the optimum filter parameter, GA is applied to noisy images for different search window. For finding out the quality of filtered image, quality metrics such as PSNR, MSE and SSIM is used. Performance of the algorithm is dependent on the optimum parameter selection.

Ali [7] proposes adaptive Weiner filter and adaptive median filter for noise removal from the MRI images. Noise considered for MRI in this book chapter is impulse and Gaussian noise. But literature related to MRI shows the indication of presence of Rician noise and not impulse or Gaussian.

Aja-Fernández and Vegas-Sánchez-Ferrero [8] proposes a case study of different modifications of LMMSE estimator filter for noise removal from MRI. They discuss the different scenario based on specific application for filter selection.

Mihaylova and Georgieva [9] discusses implementation of conventional filter such as Gaussian, Median, Wiener and Homomorphic filter available in the literature with no modification.

Sharma et al. [10] and group discusses denoising of MR images using hybrid technique based on Sylvester-Lyapunov equation and non local means method. Efficiency of this method is discussed by using only PSNR and SSIM.

Granata et al. [11] worked on implementation of non local mean filter using GPU hardware architecture to speed up the denoising procedure. But the algorithm used is original Non Local Mean algorithm.

Kuppusamy et al. [12] modified non local mean filter by changing the weight factor. In literature, the weight factor is considered as variance or multiplicative of same but in this they made it as an image adaptive value.

From the literature, it is observed that nonlinear filter is best in case of noise removal from MR image data. Nonlinear filter chosen for experiment purpose are bilateral and NLM filter. Further the NLM filter is modified which shows the clear improvement of the result over conventional bilateral and NLM filter. By adjusting the weight and normalization factor in the original NLM, results can be improved related to edge and structuring details.

2. Proposed Work

Let V be the voxel and let $g = \{f(u) | u \in V\}$ be a noisy version. The denoised value is calculated as weighted average of the image pixel.

$$MNL(g)(v) = \sum_{u \in V} w(v, u) f(u) \tag{1}$$

where $w(v, u)$ is weight value dependent on the similarity between pixel u and v and $\sum_u w(u, v) = 1$ and the Gaussian weighted Euclidean distance between two similarity window is defined as $d(f1, f2) = \|f1 - f2\|_{2, \sigma}^2$ where σ is the standard deviation of Gaussian and $f1$ and $f2$ represent two similarity window and weight is defined as following.

$$w(u, v) = \frac{1}{N(v)} \cdot e^{-d(f1, f2)/\sigma^2} \tag{2}$$

where $N(v)$ is the normalization factor and

$$N(v) = \sum_u e^{-d(f1, f2)/\sigma^2} \tag{3}$$

Modified NLM is differing with traditional NLM in the following ways. Here we have redefined distance metric as

$$d(f1, f2) = d(f1, C(f1, f2) \cdot f2) = \|f1 - C(f1, f2) \cdot f2\|_{2, \sigma}^2 \tag{4}$$

and the definitions of the modified weights to be

$$w(u, v) = \frac{C(f1, f2)}{N(v)} \cdot e^{-d(f1, f2)/\sigma^2} \tag{5}$$

where

$$C(f1, f2) = \begin{cases} \frac{E(f1)}{E(f2)} & \text{if } f1 \neq f2 \\ 1 & \text{Otherwise} \end{cases} \tag{6}$$

where $E(V)$ denotes expected value., σ is the noise presents in the image and $E(f)$ gives ideal value. In selecting the noise level, σ should be the threshold for the normalization. Here assumption made is that if changes in the signal are on large scale basis then it is an actual signal change and if it is very small change then it is due to noise.

The flow chart of the proposed algorithm is as shown in Fig. 1.

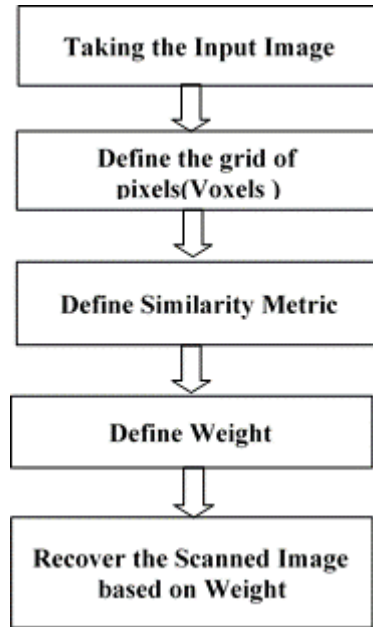


Fig. 1. Flow diagram of the proposed system.

The proposed algorithm is implemented on Spartan 6 development board with device XC6SLX9 and it is compared with conventional NLM and range domain filter. The block diagram of the proposed design is shown in Fig. 2.

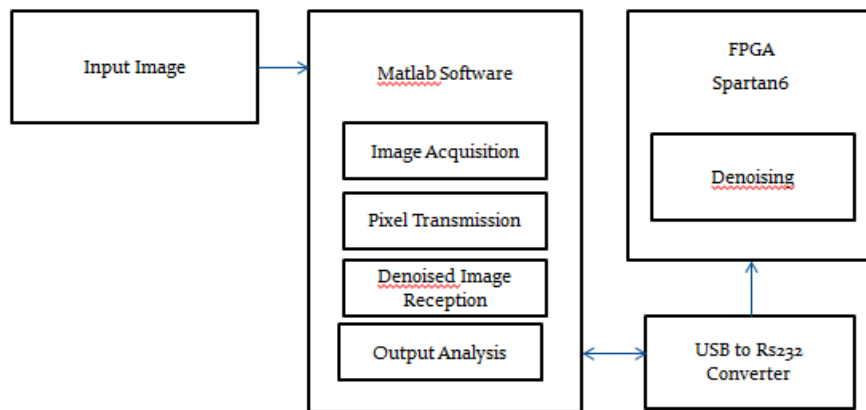


Fig. 2. Block diagram of proposed system using FPGA.

3. Results and Discussion

The database which is used for experiment purpose is downloaded from the website of University of Cyprus [13]

The database used is in TIFF format. Images used are T1 weighted brain images. The original MR-Images are de-noised using modified NLM and NLM filter and the de-noised images are as shown in Figs. 3 and 4 respectively.

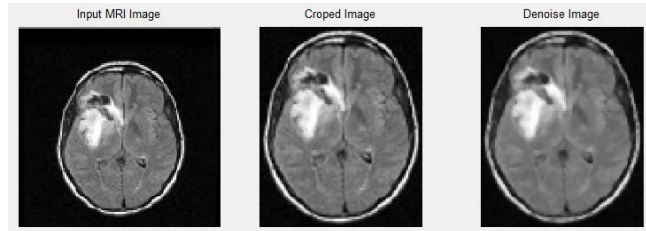


Fig. 3. Original and de-noised image using modified NLM filter.

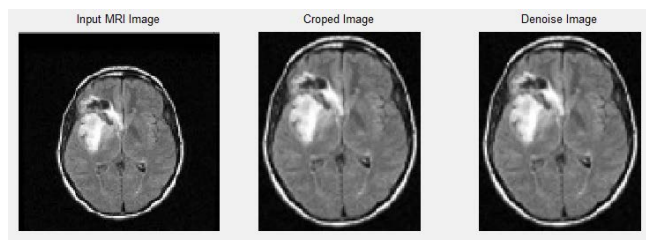


Fig. 4. Original and de-noised image using conventional NLM filter.

For subjective quality assessment ten images are shown to two radiologist, two researcher and two normal persons. The mean opinion score (MOS) calculated is as shown in Table 1 which is calculated based on the ratings received on the scale of 1 to 3 where 1 is poor and 3 is best.

Table 1. mean opinion score (MOS).

Sr. No	MOS
Image 1	2.5
Image 2	2.5
Image 3	2.333333
Image 4	2.5
Image 5	2.166667
Image 6	2.333333
Image 7	2.333333
Image 8	2.5

Various objective quality metric is also calculated related to structure and edge profile to verify the subjective assessment.

3.1. Mean squared error

The MSE is the mean squared error between the denoised and the original image, MSE is given by Eq. (7) and it is unitless quantity.

$$MSE = \frac{1}{UV} \sum_{y=1}^U \sum_{x=1}^V [|F(x, y) - F'(x, y)|^2] \tag{7}$$

where $F(x, y)$ represent the original image, $F'(x, y)$ represent the de-noised image and dimensions of the image are U and V .

SE calculated for different set of images is shown in Fig. 5.

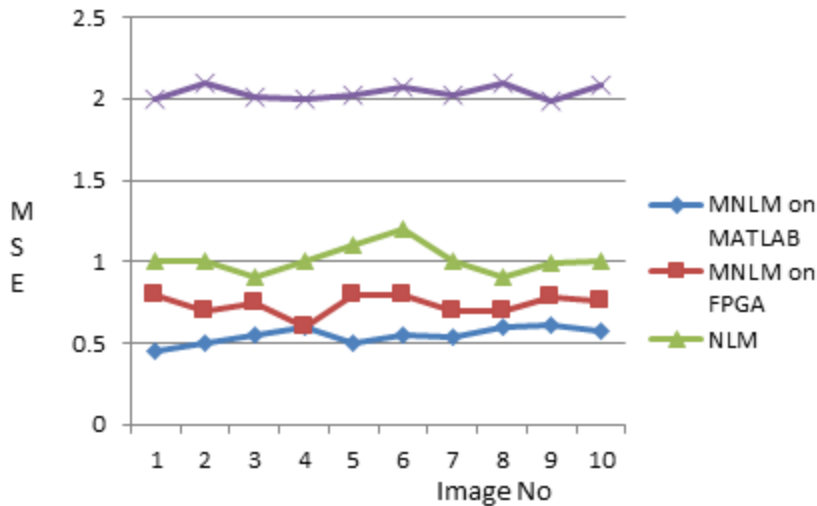


Fig. 5. Calculation of MSE.

The ideal value of mean square error (MSE) is zero and result indicates that using MNLM the value the we receive are approaching to the ideal value compared to remaining all other filters.

3.2. PSNR (Peak signal to noise ratio)

PSNR (Peak signal to noise ratio) is a ratio of signal power to the noise power that affects the quality of the resultant signal. It is calculated using a formula presented in Eq. (8). It is unitless quantity.

$$PSNR = 20 \log_{10} \frac{255}{\sqrt{MSE}} \tag{8}$$

where MSE is mean squared error. PSNR calculated for different set of images is shown in Fig. 6.

Higher the value of PSNR, it indicates better image reconstruction. This is because in the equation of PSNR, MSE is present in the denominator which should have ideal value as zero. From the graph, we can observe that the PSNR calculated for MNLM is maximum compared to all other filters considered. Even the MNLM PSNR is better than the original NLM filter which proves its better functionality over original NLM.

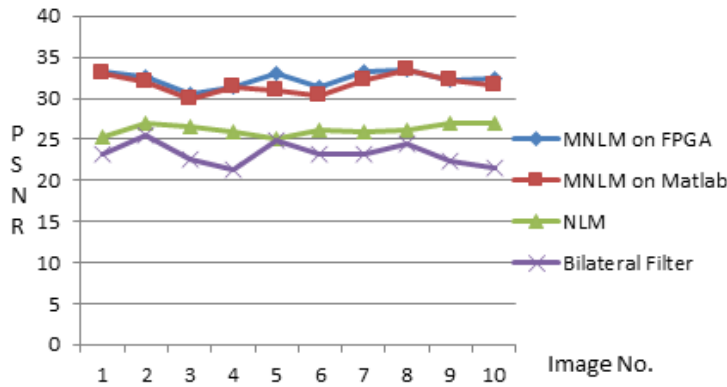


Fig. 6. Calculation of PSNR on 10 different images.

3.3. SSIM (Structural similarity index measure)

SSIM is a full reference metric. It measures the intuitive similarity between the two images. It does not judge which one is better but definitely it conclude on what is the actual structural matching between the two images. SSIM is based on visible structure in the image whereas PSNR and MSE does not depend on the visible structure. So, it is useful for finding out the structural similarity between original image and denoised image. The SSIM is calculated for different window of size M×N. Let the two windows be x and y then SSIM is given by Eq. (9). It is unitless quantity.

$$SSIM(x, y) = \frac{(2\mu_x\mu_y + c_1)(2\sigma_{xy} + c_2)}{(\mu_x^2 + \mu_y^2 + c_1)(\sigma_x^2 + \sigma_y^2 + c_2)} \tag{9}$$

where, μ_x and μ_y are average of x and y, σ_x and σ_y are the two standard deviations of x and y windows and σ_{xy} is the covariance between x and y window. c_1 and c_2 are two constants. M×N size chosen for calculation of SSIM is 4×4. SSIM calculated for different set of images is shown in Fig. 7

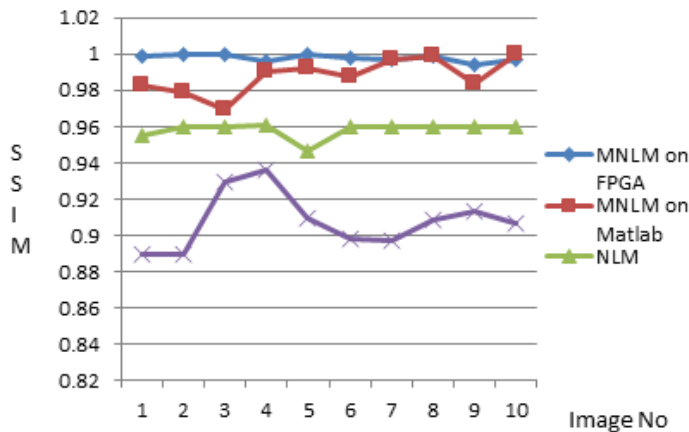


Fig. 7. Calculation of SSIM on 10 different images.

Ideal value of SSIM is 1 and for modified NLM filter the value obtained is near to 1 and it is consistent compared to conventional NLM and range domain filter.

3.4. Effect of noise variation on single image

Figure 8 shows that there is a gradual decrease in SSIM as noise varies from 1% to 11%. MNLM removes noise very effectively when noise level is up to 5% but as noise level increases, its performance goes on decreasing in terms of SSIM.

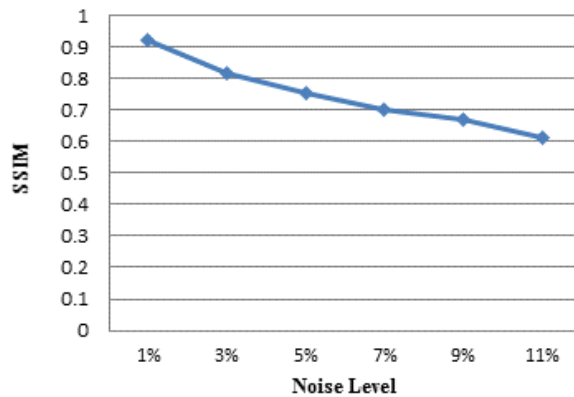


Fig. 8. SSIM calculated with variation in noise level.

3.5. PFOM (Pratt figure of merit)

PFOM is used as a performance measure in edge detection. In case of MR images for diagnostic purpose, edges play a very important role, so calculation of a performance measure which is related to edges is highly essential. PFOM (Pratt's figure of merit) [14] is given by

$$PFOM = \frac{1}{I_N} \sum_{i=1}^{I_A} \frac{1}{1+ad^2} \tag{10}$$

PFOM calculated for different set of images is shown in Fig. 9.

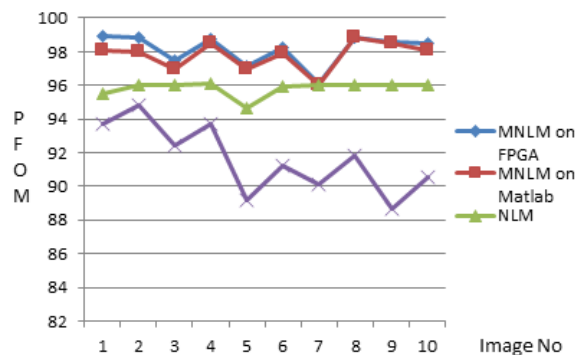


Fig. 9. Calculation of PFOM on 10 different images.

This measure is useful in comparing quality of reproduced edges in the denoised image. It conveys information about how faithfully we have generated edge profile map in the resultant image. Results obtained clearly indicate that MNLM is able to generate 100% accurate edges in the resultant image compared to remaining all other algorithms.

3.6. Correlation

Correlation gives linear relationship between two variables. It conveys the information about the matching or non matching between the two variables. Here the two variables considered are the pixel values of two images -original and denoised image. If the pixels are matching with each other or they are closed related then the correlation value will be 1. If correlation coefficient is 0, it indicates that there is no linear relationship between the variables. Correlation is given by a formula presented in Eq. (11). It is a unitless quantity.

$$CR = \frac{\sum_{i=1}^n (R_i - \bar{R}) \cdot (S_i - \bar{S})}{\sqrt{\sum_{i=1}^n (R_i - \bar{R})^2 \cdot \sum_{i=1}^n (S_i - \bar{S})^2}} \tag{11}$$

where R is the pixel value of original image and \bar{R} is the mean of original image and S is the pixel value in denoised image whereas \bar{S} is the mean of denoised image. Correlation calculated for different set of images is shown in Fig. 10. Correlation graph shows very consistent results for modified NLM filter.

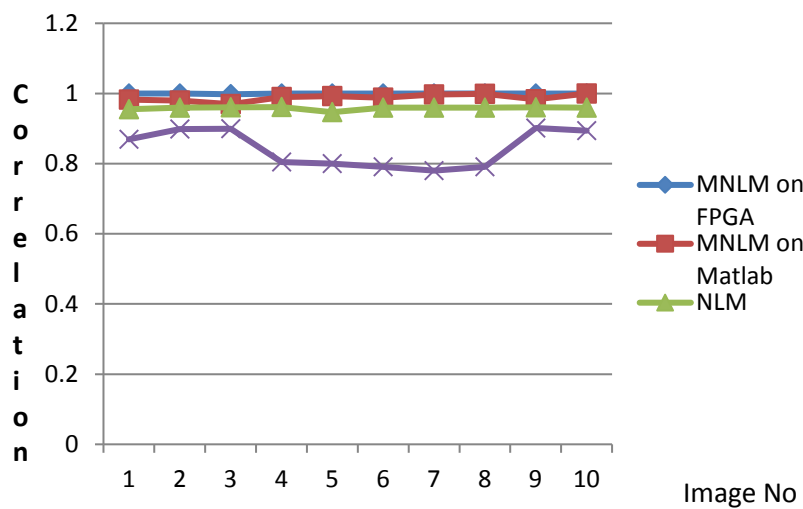


Fig. 10. Calculation of Correlation on 10 different images.

3.7. Homogeneity

Homogeneity is defined using gray level co-occurrence matrix. The gray level co-occurrence matrix is particularly suitable for describing micro texture. MRI has micro texture, which is essential for diagnostic purpose, so homogeneity is also calculated using Eq. (12).

$$\sum i, j = \frac{p(i, j)}{1 + |i - j|} \tag{12}$$

Homogeneity calculated for different set of images is shown in Fig. 11. Homogeneity calculated for modified NLM is very consistent for all 50 image set compared to others.

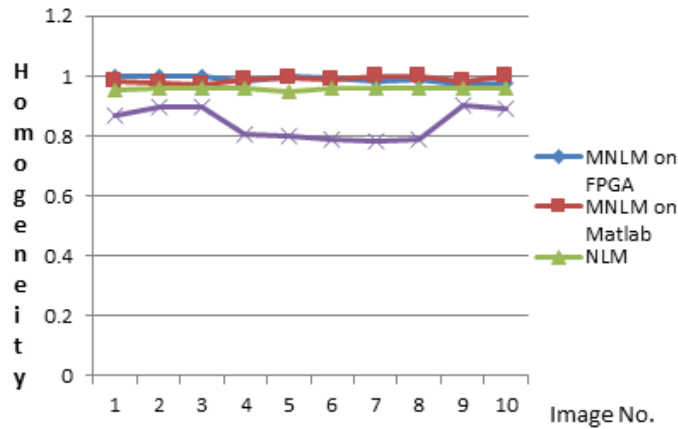


Fig. 11. Calculation of Homogeneity on 10 different images.

3.8. Energy

Energy is also defined using gray level co-occurrence matrix and is mathematically given by Eq. (13).

$$E = \sum_i \sum_j P^2(i, j) \tag{13}$$

Energy calculated for different set of images is shown in Fig. 12. From this figure, it is concluded that energy result for modified NLM is better compared to all other.

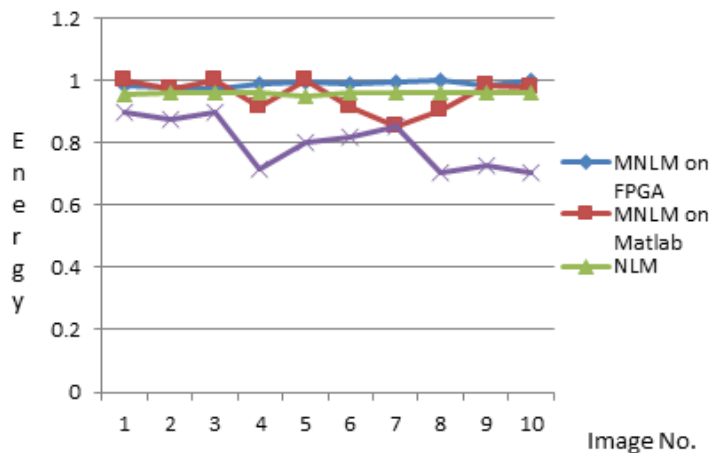


Fig. 12. Calculation of Energy on 10 different images.

3.9. Processing time

Conventional NLM filter, range domain filter and proposed filter all are implemented on Matlab as well as on FPGA and time is calculated to denoise the total image. Figure 13 shows the time utilized by Matlab is in seconds whereas time

utilized by Spartan 6 board is in milliseconds which shows a significant difference if we implement it on hardware.

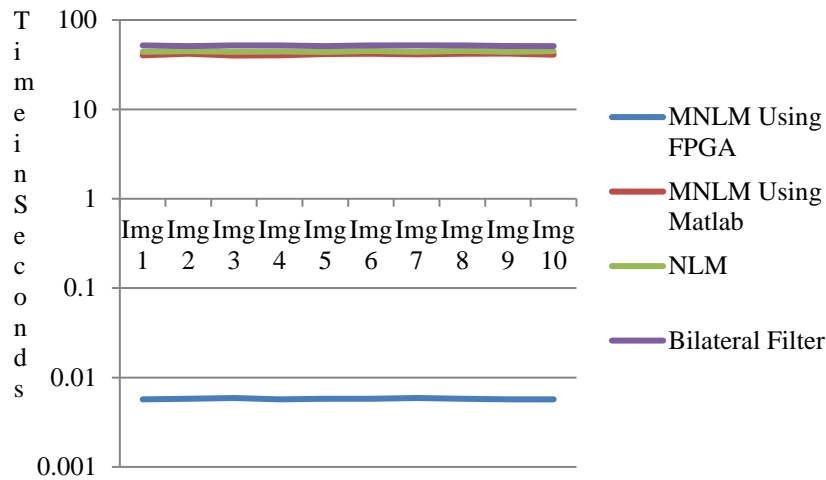


Fig. 13. Time utilized by Matlab and by FPGA.

3.10. Device utilization summary

The hardware utilization can be seen from the Table 2. LUT utilization percentage is 1% and IOB’s utilization percentage 6%. Both PSNR and MSE metric convey the information present in the image. Ideally higher the PSNR and lower the MSE conveys good retention of information. Here we have achieved best values in case of PSNR as well as MSE for MNLM filter implementation compared to other all. So, we can safely conclude that information retention in case of MNLM implementation is maximum. Homogeneity and SSIM conveys the information related to structure retention. In MNLM implementation, we are getting maximum value for the both metric approaching ideal one. This observation can lead us to the conclusion that there is no structural loss in the filtered image. PFOM gives us the information regarding recovering the edge data. For PFOM reading too, MNLM gives the maximum response leading to a conclusion that edge retention is maximum in case of MNLM filter implementation.

Table 2. Hardware utilization summary.

Logic Utilization	Used	Available	Utilization, %
Number of Slice Registers	46	11440	0
Number of Slice LUTs	76	5720	1
Number of Fully Used LUT FF Pairs	41	81	50
Number of Bonded IOBs	13	200	6

4. Conclusion

The main purpose of the work is to denoise the image without disturbing the original structure and maintaining the edge profile which is important for diagnosis purpose. New algorithm namely Modified Non Local Mean filter is proposed which shows

better qualitative and quantitative results compared to bilateral filter and conventional NLM filter. Quantitative metrics such as SSIM and PFOM related to edge and structural information shows values near to ideal value. Both subjective and objective measures suggest the better image quality in MNLM implementation. Also due to hardware implementation on FPGA, time needed to denoise the image is very less compared to its Matlab implementation. Also, device hardware utilization is optimum. The implemented hardware may be used as a hardware accelerator (HWA) in MRI machine which will generate clean image within minimum time.

5. Future Scope

For tumour detection and classification, first step is pre-processing of MR image. If image is corrupted by noise then segmentation and classification algorithm may give incorrect result. To avoid this, the first step necessary is that input image should be clean. Using the proposed algorithm, we can get clean image which can be further useful for classifier. Results are obtained with speckle noise too. Results for speckle noise are not so promising at this stage but with certain modification in the normalization factor and weight factor, we can get improved result and the same set up will be useful for removal of speckle noise from another image database.

Nomenclatures

d	Euclidean distance
f	Input Image to filter
f1, f2	Similarity Window
g	Filtered Image
$MNL(g)(v)$	Modified non local filtered pixel intensity g for image voxel v
N	Normalization constant
V	Image voxel
w	Weight
Greek Symbols	
σ	Standard deviation

Abbreviations

FPGA	Field Programming Gate Array
HWA	Hardware Accelerator
MNLM	Modified Non Local Mean
MOS	Mean Opinion Score
MRI	Magnetic Resonance Imaging
MSE	Mean Squared Error
NLM	Non Local Mean
PSNR	Peak Signal to Noise Ratio
SSIM	Structural Similarity Index Measure
PFOM	Pratt Figure Of Merit

References

1. Caverly, R.H. (2015). MRI fundamentals : RF aspects of magnetic resonance imaging(MRI). *IEEE Microwave Magazine*, 16(6), 20-33.

2. Mohan, J.; Krishnaveni, V.; and Guo, Y. (2014). A survey on the magnetic resonance image denoising methods. *Biomedical Signal Processing and Control*, 9, 56-69.
3. Tomasi, C.; and Manduchi, R. (1998). Bilateral filtering for gray and color images. *Proceedings of the Sixth International Conference on Computer Vision*. Bombay, India, 839-846.
4. Buades, A.; Coll, B.; and Morel, J.M. (2005). A review of image denoising algorithms, with a new one. *Multiscale Modeling and Simulation*, 4(2), 490-530.
5. Elahi, P.; Beheshti, S.; and Hashemi, M. (2014). BM3D MRI denoising equipped with noise invalidation technique. *Proceedings of the IEEE International Conference on Acoustics, Speech and Signal Processing (ICASSP)*. Florence, Italy, 6612-6616.
6. Akar, S.A. (2016). Determination of optimal parameters for bilateral filter in brain MR image denoising. *Applied Soft Computing*, 43, 87-96.
7. Ali, H.M. (2018). *MRI medical image denoising by fundamental filters, high-resolution neuroimaging-basic physical principles and clinical applications*, Ahmet Mesrur Halefoglul, IntechOpen.
8. Aja-Fernández, S.; and Vegas-Sánchez-Ferrero, G. (2016) *Noise filtering in MRI, Statistical analysis of noise in MRI*. Springer, Cham, 89-119.
9. Mihaylova, A.; and Georgieva, V. (2016). Comparative analysis of various filters for noise reduction in MRI abdominal images. *International Journal "Information Technologies & Knowledge"*, 10(1), 47-66.
10. Sharma, K.K.; Gurjar, D.; Jyotyana, M., and Kumari, V. (2019). *Denoising of brain MRI images using a hybrid filter method of Sylvester-Lyapunov equation and non local means*, *Smart innovations in communication and computational sciences*. Springer, Singapore, 495-505.
11. Granata, D; Amato, U. and Alfano, B. (2019). MRI denoising by nonlocal means on multi-GPU. *Journal of Real-Time Image Processing*, 16(2), 523-533.
12. Kuppusamy, P.G; Joseph, J.; and Jayaraman, S. (2019). A customized nonlocal restoration schemes with adaptive strength of smoothening for magnetic resonance images. *Biomedical Signal Processing and Control*, 49,160-172.
13. MRI Lesion Segmentation Database, Department of Computer Science, University of Cyprus. Retrieved August 11, 2020, from <http://ehealthlab.cs.ucy.ac.cy/index.php/facilities/32-software/218-datasets>
14. Abdou, I.E.; and Pratt, W.K. (1979). Quantitative design and evaluation of enhancement/thresholding edge detectors. *Proceedings of the IEEE*, 67(5), 753-763.